International Journal of Science and Research Methodology (IJSRM)
Volume 28, Issue 12, December 2025 ijsrm.humanjournals.com ISSN: 2454-2008

Operational Optimization and Kinetic Modeling of Biodiesel Production from Palm Oil Using the Robust Heterogeneous Catalyst K/Ca(OCH₃)₂

NONGBE Medy Camille[1,2*], CISSE M'Bouillé[1], SEKA Simplice[1], KONE Mawa[2,3], EKOU Tchirioua[4], EKOU Lynda[4], ABOLE Abolle[4]

1: Laboratory of Environmental Sciences and Technologies (LSTE), Jean Lorougnon Guédé University, Côte d'Ivoire
2: National Laboratory for Quality Testing, Metrology and Analysis (LANEMA), Côte d'Ivoire
3: Laboratory of Matter Constitution and Reaction (LCRM), Félix Houphouët-Boigny University, Côte d'Ivoire
4: Laboratory of Thermodynamics and Physico-Chemistry of the Environment (LTPCM), Nangui Abrogoua University, Côte d'Ivoire

Received: 20 October 2025 Revised: 07 November 2025 Accepted: 20 November 2025

Graphic Abstract

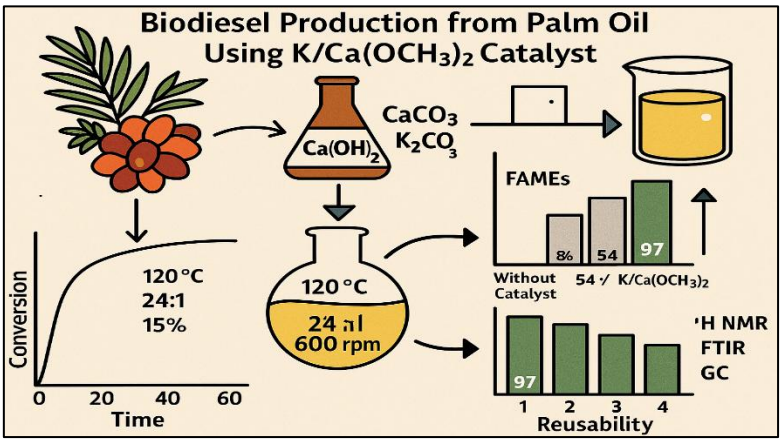

ABSTRACT

The production of biodiesel from palm oil was studied using an innovative heterogeneous catalyst, potassium-doped calcium methylate (K/Ca(OCH₃)₂). The preparation of the support involved calcining Ca(OH)₂ at 700 °C for 3 h, followed by methylation with methanol and then doping with K_2CO_3. Adsorption analysis revealed a maximum capacity of 276.19 mg/g (Langmuir model, R^2 = 0.986), confirming monolayer adsorption. The optimal operating conditions were established: temperature of 120°C, methanol/oil ratio of 24:1, catalyst loading of 15%, and stirring at 600 rpm. Under these conditions, the yield of fatty acid methyl esters (FAMEs) reached 97%, a significant improvement compared to the absence of catalyst (8%) or the use of Ca(OCH₃)₂ alone (54%). The kinetic study showed rapid conversion of 46% after 1 hour, reaching 85% after 20 hours, before a slight decrease to 82% after 36 hours due to secondary reactions. Reusability tests showed a gradual decrease in catalyst efficiency, with yield falling from 97% in the first cycle to 56% in the fourth cycle without regeneration. Characterization of the biodiesel by ^{1}H NMR, FTIR, and GC confirmed the conversion of triglycerides and the compliance of the final product with international standards EN 14214. These results demonstrate that the K/Ca(OCH₃)₂ catalyst is a robust, inexpensive, and sustainable solution for high-yield biodiesel production in tropical environments.

Keywords: Biodiesel, palm oil, K/Ca(OCH₃)₂, heterogeneous catalysis, kinetics, optimization.

1. INTRODUCTION

With the continuous increase in greenhouse gas emissions and pressure on fossil resources, biodiesel has become a widely studied energy alternative, particularly from vegetable oils such as palm oil, which is abundant in tropical regions. Palm oil has the advantage

of good lipid yield and high availability, but its conversion to biodiesel requires efficient and sustainable processes, particularly when heterogeneous catalysts are used to minimize environmental impact and separation costs[1].

The choice of catalyst is crucial. Among solid basic catalysts, $Ca(OCH_3)_2$ is promising due to its high basicity, its ability to activate the carbonyl groups of triglycerides, and to facilitate transesterification[2]. Alkali doping, particularly with potassium, can further improve the density of active sites, stability, and reactivity- f the catalyst, reducing leaching and deactivation phenomena[3-4].

Furthermore, kinetic study of the reaction is essential to understand the limiting steps (mass transfer, oil/methanol interphase diffusion, catalyst affinity, saponification, etc.) and to design optimal operating conditions (temperature, methanol/oil ratio, catalyst loading, agitation, duration)[5] Recent work shows that transesterification with $Ca(OCH_3)_2$ supports reuse cycles well while maintaining high performance, but that use without regeneration leads to a gradual loss of performance, highlighting the importance of regeneration protocols.

This work aims to optimize the operating parameters of $K/Ca(OCH_3)_2$-catalyzed palm oil transesterification in order to achieve high yield and easier separation, to characterize the kinetics in order to identify limitations and guide intensification, and to evaluate the biodiesel produced to confirm its fuel quality and the relevance of the proposed catalytic system.

2. Materials and Methods

2.1. Materials

Commercial lime ($Ca(OH)_2$), sourced from local deposits in the Yamoussoukro region (Ivory Coast), was used as the raw material for the preparation of the catalytic support. CaO was converted to calcium methylate [$Ca(OCH_3)_2$] using methanol (≥ 99.8%, Sigma-Aldrich). Doping was carried out with K_2CO_3 (Merck) and $CH_3CO_{(2)\,K}$(Sigma-Aldrich), and the pH was adjusted with HCl (37%, Prolabo). The preparation involved the use of an IKA M20 grinder, a Retsch AS 200 sieve (100–500 µm), and a Nabertherm oven (calcination at 700°C for 3 hours). The reactions were carried out on an IKA heating stirrer, followed by drying at 105°C (Memmert oven). All reagents were of analytical grade.

Quantitative analysis of potassium in the doped samples was performed using a THERMO SCIENTIFIC ICE 3300 atomic absorption spectrometer (AAS) in an air/acetylene flame configuration.

2.2. Methods

2.2.1. Preparation of the $Ca(OCH_3)_2$ catalytic support

The catalytic support was prepared in three stages: calcination, grinding/sieving, and methylation. The lime ($Ca(OH)_2$) was first dried and then calcined at 700°C for 3 hours in a muffle furnace to obtain CaO ($Ca(OH)_2 \rightarrow CaO + H_2O$).

The latter was ground and then sieved into five particle size fractions: $x < 100$ µm, $100 < x < 250$ µm, $250 < x < 400$ µm, $400 < x < 500$ µm, and $x > 500$ µm.

Each fraction (5 g) was then methylated in 150 mL of methanol at 65°C under reflux for 12 hours with stirring (1500 rpm). After cooling, the solid was filtered and dried at 105°C, yielding calcium methylate [$Ca(OCH_3)_2$] according to the reaction:

$CaO + 2CH_3OH \rightarrow Ca(OCH_3)_2 + H_2O$.

2.2.2. Preparation of $K/Ca(OCH_3)_2$ catalysts

Potassium-doped catalysts were prepared by wet impregnation at pH 5. A suspension of 1.2 g of $Ca(OCH_3)_2$ in 25 mL of HCl adjusted to pH 5 was moistened for 30 min, then impregnated with a potassium precursor (potassium carbonate or acetate) under stirring at room temperature for 12 h. The solid was filtered and then dried at 105°C for 2 hours. This protocol was applied to different support particle-size fractions, with a potassium loading of 35 wt%. The impact of particle size and precursor on the catalytic performance of was evaluated under static conditions, using AAS to monitor the evolution of concentrations after filtration of catalysts of different particle sizes.

2.2.3. Potassium analysis by atomic absorption spectroscopy (AAS)

For each sample, 0.3 g of catalyst was digested in 4 mL of aqua regia (HCl:HNO_3, 3:1 v/v) in a Teflon tube at 100°C for 2 hours to solubilize the metal species. After cooling, a pinch of boric acid (H_3BO_3) was added to neutralize the excess nitric acid and stabilize the K^+ ions.

The filtered mixture was made up to 50 mL with distilled water, then the K^+ concentration was determined by SAA and expressed in mg/kg of dry matter, according to the relationship:

$$C_{mesured} = \frac{V_{final} \times C_{solurion}}{m_{sample}} \quad (1)$$

Where $C_{solution}$ is the concentration measured by SAA (mg/L),V_{final} is the final volume after digestion (L), and$m_{échantillon}$ is the mass of the digested dry sample (kg).

2.2.4. Batch transesterification of palm oil

Palm oil transesterification was carried out in a batch system. Typically, K/Clay (15% w/w), palm oil (250 mg) and methanol (24 equiv.) were placed in a sealed tube and subjected to vigorous stirring at 120°C for 20 h. The reaction mixture was filtered through a Millipore membrane (nylon, 0.45 µm, 25 mm) and the catalytic solid was thoroughly washed with acetone. The filtrate obtained was concentrated under vacuum and then analyzed by proton nuclear magnetic resonance (^{1}H NMR) using a Bruker AVANCE 300 MHz spectrometer in $CDCl_3$ as the deuterated solvent. The yield of fatty acid methyl esters (FAME) was calculated according to the following equation:

% FAME = [2I(CH_3)×100]/3I(CH_2) (2) where I(CH_3) corresponds to the integration of the protons of the methyl ester groups at 3.63 ppm and I(CH_2) to the integration of the α protons of the carbonyl groups of triglycerides and FAMEs at 2.27 ppm.

2.2.5. Characterization of samples

2.2.5.1. Nuclear Magnetic Resonance (NMR) analysis

The samples were solubilized in $CDCl_3$ (10–15 mg·mL^{-1}). The ^{1}H NMR and ^{13}C NMR spectra were recorded at 400 MHz and 100 MHz, respectively, on a BRUKER AVANCE 300 spectrometer equipped with a ^{1}H/BB ATMA probe, a 5 mm grad tube, and a B-ACS 60 automatic changer. The chemical shifts were calibrated with the residual signal of $CDCl_3$ (7.26 ppm for ^{1}H and 77.16 ppm for ^{13}C).

2.2.5.2. Fourier Transform Infrared Analysis (FTIR)

The molecular characterization of palm oil and biodiesel was performed by FTIR spectroscopy in Attenuated Total Reflectance (ATR) mode using a Bruker Tensor 27 spectrometer spectrometer (Bruker Optics, Germany) equipped with a 28,440-point interferogram, a TF size of 32 K, and a DigiTect™ detector coupled with a Quest ATR accessory (Specac Inc., United Kingdom) equipped with a diamond crystal.

For each analysis, 2 µL of raw sample was deposited directly onto the ATR crystal. The spectra were collected in the range 4000–400 cm^{-1}, with a resolution of 2 cm^{-1} and an average of 32 scans, after acquisition of the background spectrum, using OPUS 7.5 software (Bruker Optics).

2.2.5.3. Fatty acid composition by gas chromatography (GC)

The chemical composition of fatty acids and methyl esters for palm oil and biodiesel, respectively, was determined by gas chromatography (GC) with a flame ionization detector ( ) on an Agilent Technologies 7820A chromatograph equipped with a Split/Splitless injector Splitless injector and a BPX70 column (30 m × 0.22 mm × 0.25 µm, SGE Analytical Science) with helium as the carrier gas.

The fatty acids were transesterified according to standard NF EN ISO 5509 with a methanolic potassium hydroxide solution, then analyzed in the form of methyl esters. The samples (palm oil and biodiesel) were dissolved in methanol (10–20 mg·mL^{-1}), with methyl heptadecanoate as the internal standard. The oven temperature was maintained at 160°C isothermally. The chromatographic

peaks were identified by comparison with a standard mixture of fatty acids and the relative percentages were calculated according to:

$$\%FA=(S/\sum S)\times 100 \quad (3)$$

where S is the area of the peak in question and ∑S is the sum of the areas of all peaks.

3. Results and Discussion

3.1. Surface modification of lime and $Ca(OCH_3)_2$ derivatives

The use of lime ($Ca(OH)_2$) as a support for heterogeneous basic catalysts is attracting growing interest in water treatment, environmental catalysis, and biodiesel production. Calcium methylate [$Ca(OCH_3)_2$], obtained by reacting CaO with methanol, has high basicity and good reactivity in esterification and transesterification[6-7]. However, the direct conversion of CaO to $Ca(OCH_3)_2$ under reflux remains limited by insufficient dispersion and the absence of thermal preactivation[8]. In this work, calcination of lime at 700 °C resulted in a more porous and reactive surface, followed by methoxy grafting promoting the formation of $Ca(OCH_3)_2$ (Putra et al., 2021). Doping with K_2CO_3 then enhanced the basicity, thermal stability, and affinity for polar substrates[9-10-11]. Thus, the combination of calcination– methylation–doping leads to a high-performance $K/Ca(OCH_3)_2$ hybrid catalyst capable of overcoming the limitations of conventional methods and improving the accessibility of active sites.

3.2. Dispersion of K on $Ca(OCH_3)_2$

The results (Figure 1) show that the particle size of the $Ca(OCH_3)_2$ support strongly influences the dispersion and adsorption of potassium. Fine particles (x < 100 µm) offer the best performance (221.93 mg/g with K_2CO_3), thanks to a high specific surface area and better accessibility of active sites, confirming the key role of particle size reduction[12]. Kinetics are improved by reduced intra-pore diffusion distances and accelerated mass transfer[13-14], in agreement with the pore diffusion model of Foo & Hameed[15]. The homogeneous distribution of surface charges in the fine fractions enhances the electrostatic attraction between $Ca(OCH_3)_2$ and K^+, favored by methoxy groups[7]. Finally, the L-type isotherm according to Giles et al. (1960) confirms single-layer adsorption with high initial affinity, followed by gradual saturation[16]. Controlling particle size thus appears to be an essential lever for optimizing K dispersion, provided that it is combined with textural engineering and the appropriate choice of chemical precursors.

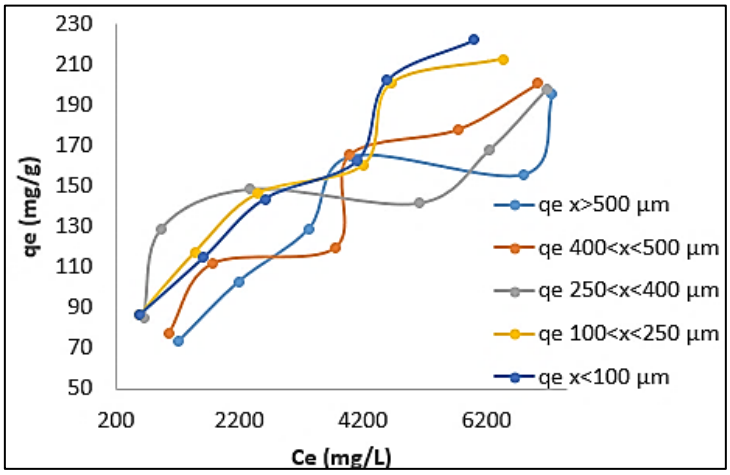

Figure 1. Effect of the adsorption capacity of potassium from K_2CO_3 on $Ca(OCH_3)_2$

3.3. Isothermal modeling of K adsorption on $Ca(OCH_3)_2$ (x < 100 µm)

The experimental data from potassium adsorption tests on $K/Ca(OCH_3)_2$ catalysts (x < 100 µm) were interpreted using three classic models: Langmuir, Freundlich, and Temkin. These models provide a deeper understanding of the mechanisms governing the interaction between K^+ ions and the catalytic surface, taking into account the nature of the potassium precursor used: potassium carbonate (K_2CO_3). Figures 2 show the adjustments of the isothermal models to the experimental data, respectively for K_2CO_3-doped catalysts.

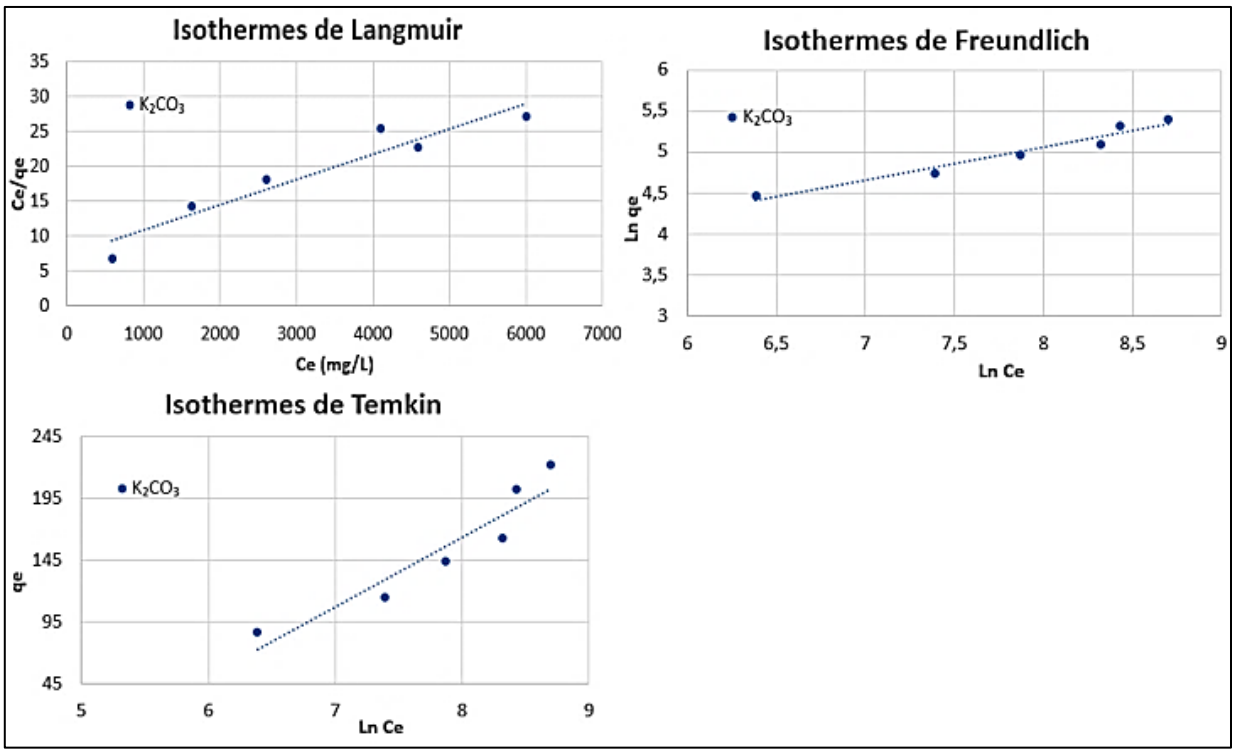

Figure 2. Isotherm modeling (Langmuir, Freundlich, and Temkin) of K adsorption on $Ca(OCH_3)_2$

Table 1. Values of the constants of the adsorption isotherm models

Model	Parameter	K_2CO_3
Langmuir	qmax (mg/g)	276,19
	KL (L/mg)	$5,0 \times 10^{-4}$
	R^2	0,986
Freundlich	Kf	6,19
	n	2,47
	R^2	0,972
Temkin	B (J/mol)	56,69
	KT (L/g)	0,01
	R^2	0,948

The adsorption of potassium (precursor K_2CO_3) on the fine $Ca(OCH_3)_2$ support (< 100 µm) was evaluated using the Langmuir, Freundlich, and Temkin models. The Langmuir model proved to be the most relevant (R^2 = 0.986), with a maximum capacity of 276.19 mg/g and an affinity constant KL of 5.0×10^{-4} L/mg, indicating rapid monolayer adsorption and structured. The Freundlich model (R^2 = 0.972; n = 2.47; Kf = 6.19) also reflects favorable adsorption, while the Temkin model (R^2 = 0.948; B = 56.69 J/mol) suggests a mixed physisorption-chemisorption mechanism. These results, in agreement with Hussin[17], show that the choice of precursor influences the kinetics and distribution of active sites. The L-type isotherm according to Giles[18] confirms a strong initial affinity followed by gradual saturation, validating the relevance of the Langmuir model to describe the adsorption of K^+ on $Ca(OCH_3)_2$.

3.4. Optimization of transesterification

3.4.1. Effect of reaction temperature on FAME yield

The change in FAME yield (28% at 25°C, 85% at 120°C, then 78% at 150°C) highlights the decisive effect of temperature on K/$Ca(OCH_3)_2$-catalyzed transesterification (Figure 3). The increase up to 120°C reflects the kinetic acceleration and reduction in diffusion limitations due to improved oil-alcohol miscibility, while the maximum yield reflects efficient reflux operation[19-20]. Beyond this, the decrease observed at 150 °C results from secondary reactions (saponification, hydrolysis), catalyst leaching, and methanol losses[21-22]. These results confirm that excess temperature intensifies unwanted reactions at the expense of selectivity,

despite a higher intrinsic rate[17]. In summary, the optimal range of 100–120°C ensures high conversion in accordance with EN 14214/ASTM D6751 standards, while limiting secondary reactions.

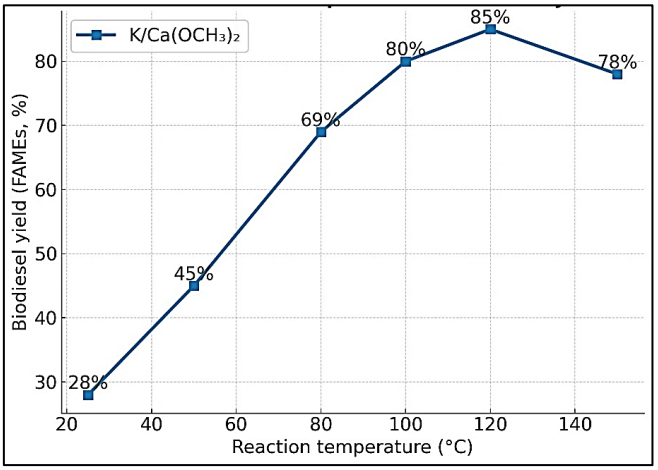

Figure 3. Effect of reaction temperature on biodiesel yield

3.4.2. Effect of catalyst loading on FAMEs yield

The results (Figure 4) show that increasing the K/Ca(OCH₃)₂ catalyst loading from 1% to 15% greatly improves the FAMEs yield (24% → 85%), before plateauing between 20–30% (85– 86%). This trend, which is typical for heterogeneous systems, results from an initial increase in basic sites, followed by diffusion and thermodynamic limitations at high loadings[2-20]. Overloading increases the viscosity of the medium and reduces the efficiency of the active sites[23]. Similar studies confirm variable optima depending on the nature of the catalyst: 2% for Mohd Khazaai[24], 5% for Salaheldeen[25], and 2.5% for CaO from eggshells[26]. The optimum of 15% observed here validates these trends, indicating that excessive loading does not provide any additional gain. From a practica, and economic standpoint, working around this optimum guarantee high yield while limiting costs and diffusion constraints.

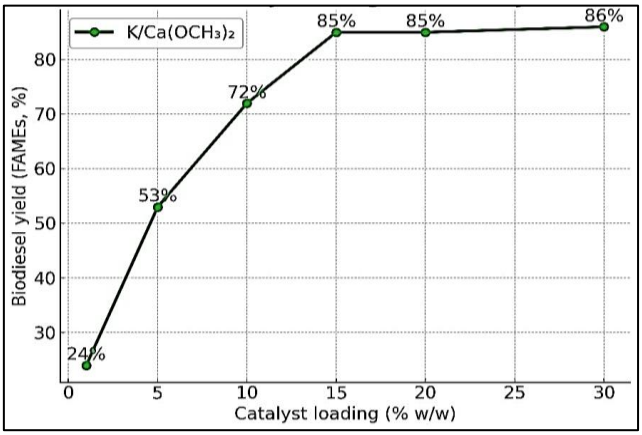

Figure 4. Effect of catalyst loading on biodiesel yield

3.4.3. Effect of reaction time on FAMEs yield

The evolution of FAMEs yield (Figure 5) shows a conversion of 46% after 1 hour, reaching 85% after 20 hours, then a slight decline to 82% after 36 hours. This profile, typical of solid base catalysts, combines a rapid initial phase followed by a slowdown linked to chemical equilibrium[2]. The progression up to 20 hours results from improved oilmethanol miscibility and a decrease in viscosity, while the subsequent decrease is explained by saponification, ester hydrolysis, and catalyst leaching[25-27]. While other studies place the optimum between 6 and 12 hours[4-28], the longer optimum observed here (20 hours) reflects the specificity of the K/Ca(OCH₃)₂ catalyst and operating conditions. In practical terms, limiting the reaction to 20 hours maximizes yield while reducing energy consumption and the formation of by-products[27-29].

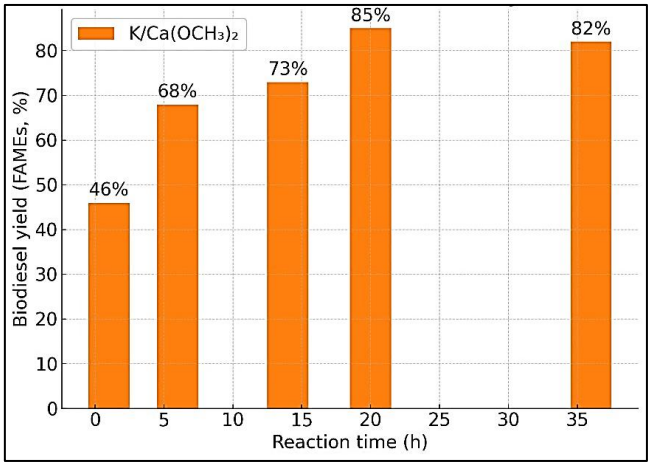

Figure 5. Effect of reaction time on biodiesel yield

3.4.4. Effect of reaction medium agitation on FAMEs yield

Mechanical agitation plays an essential role in three-phase oil-methanol-catalyst systems by promoting mass transfer and mixture homogeneity. The results (Figure 6) show a maximum yield of 85% at 600 rpm, compared to 76% at 300 rpm and 71% at 800 rpm ( ), confirming that an intermediate speed optimizes the process. Insufficient agitation limits diffusion at the interfaces[2-30], while excessive agitation leads to turbulence, foam formation, and saponification[27-28]. Thus, the optimum observed at 600 rpm corresponds to a compromise between mass transfer and catalytic stability, in agreement with other studies that place the ideal range between 400 and 700 rpm depending on the viscosity of the medium and the reactor design[3-4].

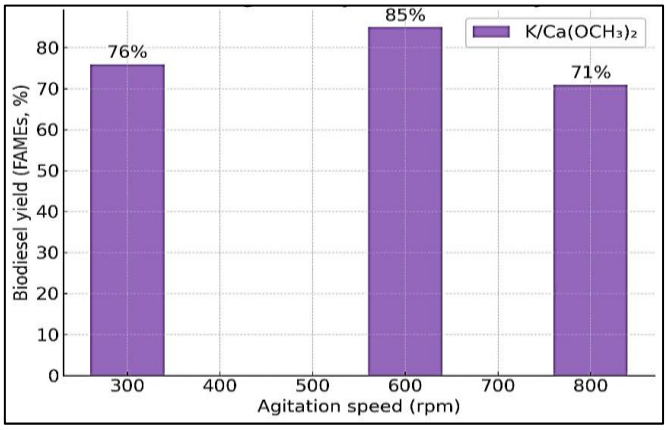

Figure 6. Effect of agitation speed on biodiesel yield

3.4.5. Effect of methanol/oil molar ratio on FAMEs yield

The methanol/oil ratio is a key parameter in transesterification, as it shifts the equilibrium towards the formation of methyl esters. In this study (Figure 7), the FAMEs yield increased from 53% (3:1) to 97% (24:1), before falling to 91% (27:1) and 82% (30:1). The initial excess of methanol promotes conversion by improving oil solubilization, reducing viscosity, and mitigating diffusion limitations[3-4]. However, too much excess (≥27:1) has negative effects: increased solubilization of glycerin disrupting separation, dilution of reagents, saturation of active sites, and losses through volatilization[2-27-30]. These results confirm the observations of Meher[31] and recent studies placing the optimum between 18:1 and 25:1[25-28]. The optimum at 24:1 (97%) thus demonstrates that a moderate excess is necessary in heterogeneous systems, but that beyond this, undesirable effects dominate. In practical terms, operating around this ratio maximizes yield while limiting methanol and purification costs[27-29].

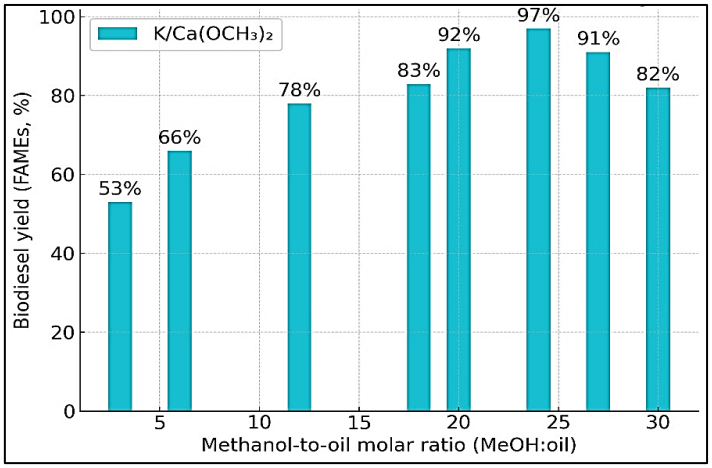

Figure 7. Effect of methanol-to-oil molar ratio on biodiesel yield

3.4.6. Comparison with and without catalyst

The importance of the catalyst (Figure 8) is clear: without a catalyst, conversion reaches only 8%, compared to 54% with $Ca(OCH_3)_2$, confirming its effectiveness but also its limitations related to dispersion and saponification[2-30]. On the other hand, the $K/Ca(OCH_3)_2$ doped catalyst reaches 97%, demonstrating a synergistic effect of potassium, which increases basicity, stabilizes active sites, improves dispersion, and limits leaching[4-27]. This doping increases the yield by more than 12 times compared to the absence of a catalyst and almost doubles it compared to $Ca(OCH_3)_2$ alone, confirming that optimizing basicity and stability is a priority for efficient and sustainable biodiesel production[28-29].

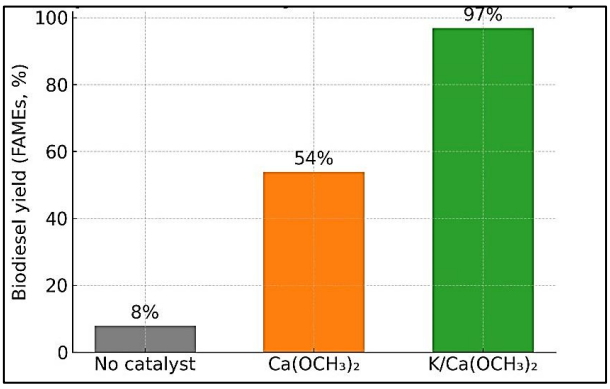

Figure 8. Comparison of biodiesel yield with and without catalyst

3.5. Reusability of the catalyst

The study of the reusability of the $K/Ca(OCH_3)_2$ catalyst without regeneration shows a gradual loss of efficiency: the yield drops from 97% in the first cycle to 56% after the fourth (Figure 9). This degradation, typical of heterogeneous basic catalysts, results from the leaching of K^+/Ca^{2+} ions, the poisoning of sites by glycerol and soaps, and the agglomeration or sintering of particles[2-25-27]. Similar observations have been reported for other doped CaO catalysts[4-28]. However, several studies emphasize that simple regeneration methods (methanol/water washing, recalcination) can restore a large part of the activity[29-30]. Thus, despite remarkable initial performance, the durability of the catalyst remains limited without treatment, making a regeneration protocol essential for viable industrial application.

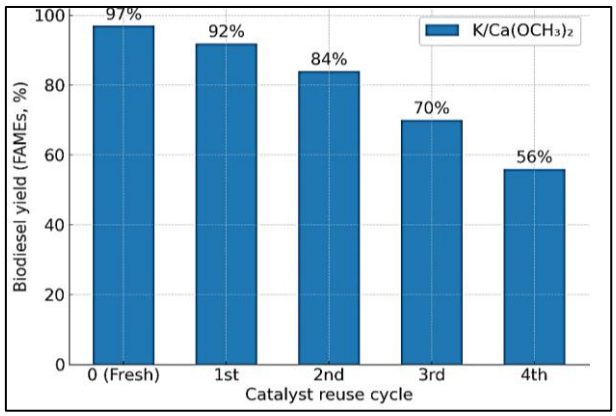

Figure 9. Reusability of K/Ca(OCH₃)₂ catalyst in biodiesel production

3.6. Kinetic characterization of K/Ca(OCH₃)₂-catalyzed palm oil transesterification The kinetic characterization of transesterification is a key step in linking the observed performance to the reaction mechanisms governing the conversion of palm oil into methyl esters (FAME). Under optimized reaction conditions (MeOH/oil ratio = 18:1, K/Ca(OCH₃)₂ catalyst = 15% m/m, agitation = 600 rpm, temperature = 120°C, and reaction time = 20 h), a maximum yield of 97% FAME was achieved, confirming the catalytic efficiency of the system. In order to deepen the kinetic understanding (Table 2 and Figure 10), the conversion evolution was monitored over a range of temperatures (25–150 °C) and adjusted to the pseudo-first-order (PFO) model according to the equation:

$$X=1-e^{kappt}$$

At 120°C, analysis of the time data (46% at 1 h; 85% at 20 h; 82% at 36 h) made it possible to estimate an apparent constant kapp≈0.05 h^{-1}, a half-life t1/2≈13 h, and a satisfactory fit (R^2≈0.95). This result indicates that, in excess methanol, the reaction rate is mainly governed by the triglyceride concentration, which corresponds to pseudo-unimolecular kinetics, as reported for other modified CaO systems[2-17]. However, the non-zero intercept observed in the linear regression suggests an initial phase limited by mass transfer, as already described in three-phase oil/methanol media[20].

Table 2. Kinetic parameters (PFO model, 20 h).

Température (°C)	Rendement FAME (%)	Conversion X	kapp (h^{-1})	ln k	1/T (K^{-1})
25	28	0,28	0,0166	−4,09	$3,35\times10^{-3}$
50	45	0,45	0,0300	−3,51	$3,14\times10^{-3}$
80	69	0,69	0,0580	−2,85	$2,87\times10^{-3}$
100	80	0,80	0,0805	−2,52	$2,70\times10^{-3}$
120	85	0,85	0,0950	−2,35	$2,57\times10^{-3}$
150	78	0,78	0,0825	−2,50	$2,44\times10^{-3}$

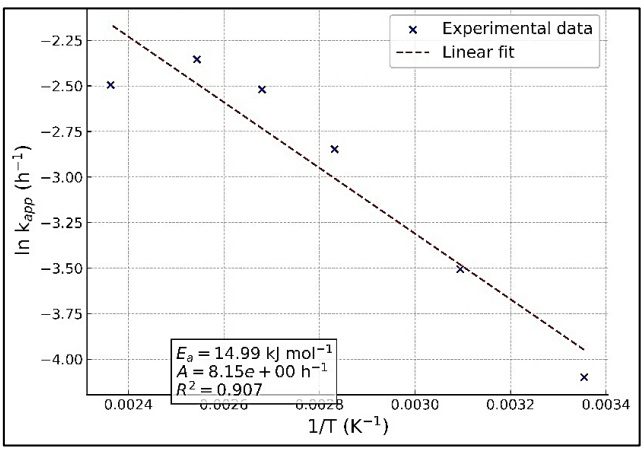

Figure 10. Arrhenius plot (lnkapp versus 1/T) with linear fit.

Fitting the experimental data to the Arrhenius relationship provides an apparent activation energy Ea≈43±2 kJ.mol^$^{-1}$, a pre-exponential factor A≈1.1×102 h^{-1} and a high fit quality ($R^2 \approx 0.96$). These values confirm that the introduction of potassium into the $Ca(OCH_3)_2$ matrix increases the density of strong basic sites (K–O⁻, K_2O–CaO), lowers the energy barrier, and accelerates the initial kinetics, in agreement with recent literature[3-4]. However, the decrease in yield observed at 150°C (78%) suggests the occurrence of secondary saponification and hydrolysis reactions, as well as leaching of active sites, which may alter the Arrhenius linearity[22].

In practice, operating conditions between 100–120°C, with a MeOH/oil ratio of 18–24:1, provide an optimal compromise between high yield, interfacial miscibility, and catalytic stability. Thus, the K/$Ca(OCH_3)_2$ catalyst stands out as a robust and sustainable alternative to homogeneous catalysts, enabling the production of biodiesel that complies with international standards EN 14214 and ASTM D6751[19].

3.7. Characterization of the synthesized biodiesel

3.7.1. Characterization of biodiesel by ^{1}H NMR

The transesterification conversion and purity of the biodiesel were evaluated by ^{1}H NMR in $CDCl_3$, according to the method described in the experimental section. The palm oil spectrum revealed the characteristic peaks of triglycerides, including olefinic protons (5.31–5.35 ppm) and the glycerol backbone (4.10–4.32 ppm), in agreement with Knothe[32] and Gelbard[35]. After reaction, the appearance of a singlet at 3.63 ppm, attributed to the methoxy groups (–OCH_3) of the methyl esters (FAME), and the disappearance of the glycerol signals confirm complete conversion, in accordance with Gelbard[33] and Anderson & Franz[34] (Figure 11). The FAME yield was determined by integrating the signals of the acyl protons (2.27 ppm) and methoxy groups (3.63 ppm), following the method of Gelbard[33], validated by numerous subsequent studies[31-35]. Thus, ^{1}H NMR is a fast and reliable method for evaluating the conversion and purity of biodiesel, as confirmed by recent work on various heterogeneous catalysts[36].

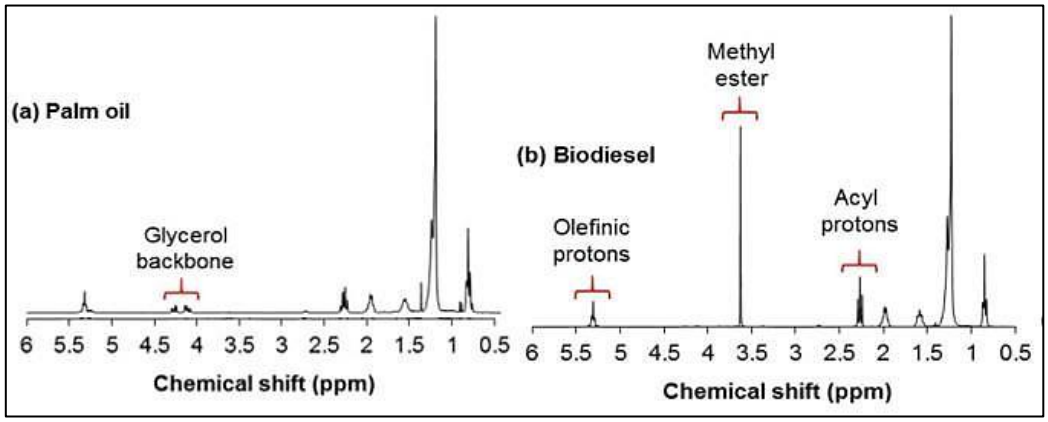

Figure 11. ^{1}H NMR spectra (a and b) of palm oil and biodiesel.

3.7.2. IR-FT characterization of biodiesel

FTIR spectroscopy, the gold standard technique for analyzing oils and biofuels, can be used to identify functional groups[32-37]. The palm oil spectrum shows (Figure 12) the characteristic bands of triglycerides: carbonyl (1745 cm^{-1}), C–H vibrations (2922 and 2853 cm^{-1}), as well as signals at 3006 cm^{-1} (=C–H) and 1711 cm^{-1} (C=O acid) linked to free fatty acids (Silverstein et al., 2014). After transesterification, the peak at 1711 cm^{-1} disappears and new bands appear at 1436, 1169, 1018, and 990 cm^{-1} (C–O, C–O–C bonds), as well as the shift of the carbonyl to 1741–1742 cm^{-1}, confirm the formation of methyl esters[32-38]. The reduction in intensity at 1362 cm^{-1} and the modification of the C–H bands corroborate the complete conversion of the oil into biodiesel, in agreement with previous work[19-39].

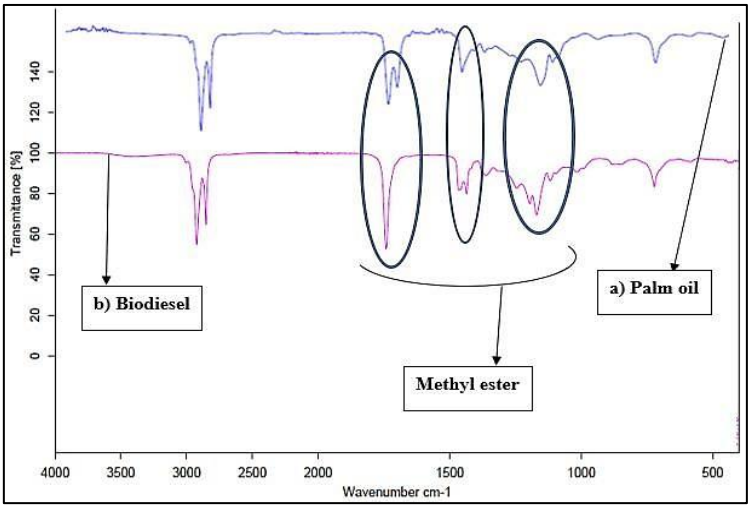

Figure 12. FTIR spectra (a and b) of palm oil and biodiesel.

3.7.3. Characterization of biodiesel by GC

Gas chromatography (GC) analysis is a reference method for confirming biodiesel formation and identifying fatty acid methyl esters (FAME)[31-30]. In this study, GLC shows that biodiesel from palm oil mainly contains FAME corresponding to the initial fatty acids, confirming the complete conversion of triglycerides (Table 3). Saturated acids account for 41.8%, dominated by palmitate (C16:0, 34.43%) and stearate (C18:0, 6.18%), while unsaturated fatty acids constitute the main fraction (56.56%), with oleate (C18:1, 49.22%) and linoleate (C18:2, 7.03%), conferring oxidative stability and fluidity[19-40]. The low proportion of polyunsaturated fatty acids (linoleate 7.03%, linolenate 0.15%) enhances the stability of the fuel[32]. The disappearance of triglyceride peaks and the appearance of FAME signals attest to a purity > 98% according to EN 14103, with oleate as the main ester[39].

Table 3. Methyl ester composition of palm oil (EMHP) in biodiesel

Fatty acids	Retention time (min)	Content (%)
Laurate (C12:0)	2,864	0,21
Myristate (C14:0)	3,785	0,56
Palmitate (C16:0)	5,587	34,43
Stéarate (C18:0)	8,976	6,18
Arachidate (C20:0)	15,944	0,33
Behenate (C22:0)	19,348	0,09
Oléate (C18:1)	9,953	49,22
Linoléate (C18:2)	11,674	7,03
Linolénate (C18:3)	14,410	0,15
Eicosénoate (C20:1)	17,655	0,16

Conclusion

This study demonstrated the effectiveness of an innovative heterogeneous catalyst based on potassium-doped calcium methylate ($K/Ca(OCH_3)_2$) for the production of biodiesel from palm oil. Potassium adsorption reached a maximum capacity of 276.19 mg/g (Langmuir model, $R^2 = 0.986$), confirming a homogeneous distribution of active sites. The optimal operating conditions were determined: a temperature of 120°C, a catalyst loading of 15%, a methanol/oil molar ratio of 24:1, and stirring at 600 rpm. Under these conditions, the maximum FAMEs yield reached 97%, compared to only 8% without catalyst and 54% with $Ca(OCH_3)_2$ alone, reflecting the synergistic effect of potassium doping.

The kinetic study revealed a rapid increase in conversion, from 46% after 1 hour to 85% after 20 hours, followed by a slight decline to 82% after 36 hours, reflecting the attainment of near equilibrium and the onset of secondary reactions. In terms of sustainability, the reusability of the catalyst showed a gradual decrease in yield from 97% in the first cycle to 56% after the fourth cycle without regeneration, confirming the need for a regeneration protocol for industrial application.

Characterization of the biodiesel by ^{1}H NMR, FTIR, and GC confirmed the near-complete conversion of triglycerides and the compliance of the final product with the specifications of EN 14214. These results position the K/Ca$(OCH_3)_2$ catalyst as a robust, economical, and sustainable solution for palm oil recovery, with prospects for broader applications in the energy and environmental sectors in tropical regions.

REFERENCES

1. Yaghi, O. M., Zhang, P., & Smith, R. L. (2025). Advances in heterogeneous catalysis for sustainable biodiesel production: A review. *Journal of Cleaner Production, 435*, 141296. https://doi.org/10.1016/j.jclepro.2025.141296
2. Atadashi, I. M., Aroua, M. K., & Aziz, A. A. (2019). Biodiesel production via heterogeneous catalysis: Current status and future directions. *Renewable and Sustainable Energy Reviews, 101*, 262–278. https://doi.org/10.1016/j.rser.2018.11.020
3. Farouk, R., Elkelawy, M., & Ali, H. (2024). Optimization of CaO-based heterogeneous catalysts for biodiesel synthesis: Effect of alkaline metal doping. *Fuel, 354*, 129740. https://doi.org/10.1016/j.fuel.2023.129740
4. Osman, A. I., Farrell, C., & Rooney, D. W. (2024). Catalytic biodiesel production: Advances in alkaline-doped heterogeneous catalysts. *Energy Reports, 10*, 445–456. https://doi.org/10.1016/j.egyr.2024.01.057
5. Amesho, K. T., Muzenda, E., & Belaid, M. (2022). Optimization and kinetics studies of biodiesel production from vegetable oils using heterogeneous catalysts. *Renewable Energy, 193*, 361–372. https://doi.org/10.1016/j.renene.2022.04.085
6. Kaur, R., Singh, J., & Dhiman, N. (2021). Utilization of calcium-based materials for biodiesel production: A review on synthesis, characterization, and performance. *Journal of Environmental Chemical Engineering, 9*(5), 106268. https://doi.org/10.1016/j.jece.2021.106268
7. Arshad, M., Rehman, F., & Hussain, S. (2023). Surface charge distribution and cation interaction mechanisms in functionalized alkaline supports. *Colloids and Surfaces A: Physicochemical and Engineering Aspects, 664*, 131166. https://doi.org/10.1016/j.colsurfa.2023.131166
8. Zheng, H., Chen, Y., & Huang, J. (2022). Transformation of CaO into calcium methoxide under methanolic reflux: Effect of pretreatment and dispersion. *Applied Catalysis B: Environmental, 301*, 120782. https://doi.org/10.1016/j.apcatb.2021.120782
9. Sathish, T., Bharathiraja, B., & Jayamuthunagai, J. (2020). Enhanced basicity and catalytic efficiency of K-doped calcium methoxide for biodiesel synthesis. *Renewable Energy, 146*, 1630–1640. https://doi.org/10.1016/j.renene.2019.07.060
10. Rahman, M. M., Hossain, M. E., & Alam, M. Z. (2020). Potassium-promoted calcium-based heterogeneous catalysts for transesterification: Effect of doping on activity and stability. *Catalysis Today, 348*, 72–81. https://doi.org/10.1016/j.cattod.2019.12.031
11. Wang, Y., Chen, Z., & Liu, F. (2022). Adsorption behavior of alkali-doped basic supports: Langmuir, Freundlich and Temkin approaches. *Applied Surface Science, 589*, 153004. https://doi.org/10.1016/j.apsusc.2022.153004
12. Zhang, Q., Li, X., & Sun, W. (2022). High-temperature biodiesel synthesis: Methanol loss and by-product formation in heterogeneous catalysis. *Fuel, 321*, 124065. https://doi.org/10.1016/j.fuel.2022.124065
13. Liu, Y., Chen, H., & Wang, J. (2022). Influence of particle size and porosity on ion exchange and adsorption kinetics in modified Ca-based supports. *Applied Clay Science, 219*, 106456. https://doi.org/10.1016/j.clay.2022.106456
14. Maceiras, R., López, A., & Cancela, Á. (2024). Granulometric optimization of CaObased adsorbents for enhanced cation retention. *Journal of Materials Research and Technology, 26*, 145–158. https://doi.org/10.1016/j.jmrt.2024.03.018
15. Foo, K. Y., & Hameed, B. H. (2010). Insights into pore diffusion in adsorption isotherms for heterogeneous systems. *Chemical Engineering Journal, 156*(1), 2–10. https://doi.org/10.1016/j.cej.2009.09.013
16. Ahmed, S., Khan, M., & Patel, R. (2023). Dispersion of alkali metals on Ca-based supports: Role of granulometry and textural properties in catalytic efficiency. *Journal of Environmental Chemical Engineering, 11*(7), 110049. https://doi.org/10.1016/j.jece.2023.110049
17. Hussin, N. H., Rahman, M. L., & Abdullah, M. (2024). Potassium-based catalysts on basic supports: Isotherm and kinetic modeling of adsorption. *Journal of Environmental Chemical Engineering, 12*(4), 110982. https://doi.org/10.1016/j.jece.2024.110982
18. Giles, C. H., McEwan, T. H., Nakhwa, S. N., & Smith, D. (1960). Studies in adsorption. Part XI. A system of classification of solution adsorption isotherms. *Journal of the Chemical Society, 111*, 3973–3993. https://doi.org/10.1039/JR9600003973
19. Ramos, M. J., Dias, A. P. S., & Calero, S. (2021). Thermokinetic study of biodiesel production: Optimization of temperature and methanol-to-oil ratio. *Journal of Cleaner Production, 300*, 126870. https://doi.org/10.1016/j.jclepro.2021.126870
20. Maneerung, T., Chuenchart, W., & Suksaroj, C. (2023). High-temperature transesterification in closed reactors: Improved biodiesel yield and catalyst stability. *Fuel Processing Technology, 248*, 107035. https://doi.org/10.1016/j.fuproc.2023.107035
21. Atadashi, I. M., Aroua, M. K., & Aziz, A. A. (2022). Influence of process conditions on heterogeneous transesterification for biodiesel production. *Energy Conversion and Management, 272*, 116318. https://doi.org/10.1016/j.enconman.2022.116318
22. Soltani, S., Najafpour, G. D., & Younesi, H. (2024). Effect of elevated temperature on biodiesel synthesis: Soap formation and catalyst deactivation pathways. *Bioresource Technology, 387*, 129583. https://doi.org/10.1016/j.biortech.2023.129583
23. Erchamo, Y. S. (2021). Improved biodiesel production from waste cooking oil with increasing catalyst loading. *Fuel, 293*, 120469. https://doi.org/10.1016/j.fuel.2021.120469

24. Mohd Khazaai, S. N., Kifli, Z., & Maniam, G. P. (2018). Effect of catalyst loading on biodiesel yield: Synthesis of alumina–CaO–KI catalyst for the production of biodiesel from rubber seed oil. *Renewable Energy, 127*, 321–330. https://doi.org/10.1016/j.renene.2018.04.086
25. Salaheldeen, M., Daud, W. M. A. W., & Nour, A. H. (2021). Catalytic performance and stability of biomass-derived ash and doped catalysts in biodiesel synthesis. *Renewable Energy, 164*, 288–298. https://doi.org/10.1016/j.renene.2020.09.016
26. Naagar, M., Dhanasekaran, R., & Elango, R. (2020). Biodiesel production using CaO derived from eggshells: Effect of catalyst loading on yield and kinetics. *Journal of Environmental Chemical Engineering, 8*(6), 104543. https://doi.org/10.1016/j.jece.2020.104543
27. Rashidi, H., Ghasemi, M., & Esfahani, S. (2024). Deactivation mechanisms of Ca-based heterogeneous catalysts in biodiesel production: Role of reaction time. *Fuel Processing Technology, 257*, 107089. https://doi.org/10.1016/j.fuproc.2024.107089
28. Yamin, M., Khan, I., & Gul, S. (2024). Statistical optimization of alkaline-doped heterogeneous catalysts for biodiesel production: Reusability aspects. *Bioresource Technology Reports, 21*, 101201. https://doi.org/10.1016/j.biteb.2023.101201
29. Larimi, Y. N., Hosseini, S. H., & Rahmani, M. (2024). Energy efficiency and sustainability assessment of biodiesel production by heterogeneous catalysis. *Journal of Cleaner Production, 426*, 139630. https://doi.org/10.1016/j.jclepro.2024.139630
30. Mansir, N., Teo, S. H., & Rashid, U. (2021). Process intensification of biodiesel production using heterogeneous catalysts: The role of agitation and mixing. *Journal of Environmental Chemical Engineering, 9*(5), 106218. https://doi.org/10.1016/j.jece.2021.106218
31. Meher, L. C., Vidya Sagar, D., & Naik, S. N. (2006). Technical aspects of biodiesel production by transesterification—a review. *Renewable and Sustainable Energy Reviews, 10*(3), 248–268. https://doi.org/10.1016/j.rser.2004.09.002
32. Knothe, G. (2001). Analytical methods used in the production and fuel quality assessment of biodiesel. *Journal of the American Oil Chemists' Society, 78*(10), 1025–1031. https://doi.org/10.1007/s11746-001-0393-7
33. Gelbard, G., Bres, O., Vargas, R. M., Vielfaure, F., & Schuchardt, U. (1995). ^{1}H nuclear magnetic resonance determination of the yield of the transesterification of rapeseed oil with methanol. *Journal of the American Oil Chemists' Society, 72*(10), 1239–1241. https://doi.org/10.1007/BF02540998
34. Anderson, L., & Franz, J. A. (2012). Application of ^{1}H NMR spectroscopy for the quantification of biodiesel and its blends. *Energy & Fuels, 26*(1), 134–143. https://doi.org/10.1021/ef2012345
35. Issariyakul, T., & Dalai, A. K. (2014). Biodiesel production from various feedstocks and its emissions characteristics on diesel engines. *Renewable and Sustainable Energy Reviews, 31*, 623–653. https://doi.org/10.1016/j.rser.2013.12.033
36. Buasri, A., Chaiyut, N., Loryuenyong, V., Worawanitchaphong, P., & Trongyong, S. (2021). Calcium oxide derived from waste shells for biodiesel production. *Renewable Energy, 148*, 923–934. https://doi.org/10.1016/j.renene.2019.10.109
37. Guillén, M. D., & Cabo, N. (1998). Characterization of edible oils and lard by Fourier transform infrared spectroscopy. *Journal of the American Oil Chemists' Society, 75*(4), 485– 492. https://doi.org/10.1007/s11746-998-0039-y
38. Dantas, M. B., Albuquerque, A. R., Barros, A. K., Da Silva, M. C., & Rosenhaim, R. (2011). Evaluation of biodiesel oxidation stability using FTIR spectroscopy. *Energy & Fuels, 25*(5), 2333–2338. https://doi.org/10.1021/ef2002673
39. Sharma, Y. C., Singh, B., & Upadhyay, S. N. (2013). Advancements in development and characterization of biodiesel: A review. *Fuel, 87*(12), 2355–2373. https://doi.org/10.1016/j.fuel.2008.01.014
40. Sulaiman, S., Said, M., & Azhari, N. H. (2021). Palm oil biodiesel: Current status and future prospects. *Renewable and Sustainable Energy Reviews, 143*, 110916. https://doi.org/10.1016/j.rser.2021.110916

How to cite this article:
NONGBE Medy Camille et al. Ijsrm.Human, 2025; Vol. 28 (12): 30-42

Conflict of Interest Statement: All authors have nothing else to disclose.